Ther Adv Chronic Dis
2020, Vol. 11: 1–17
DOI: 10.1177/2040622320962648

Poricoic acid A as a modulator of TPH-1 expression inhibits renal fibrosis *via* modulating protein stability of β-catenin and β-catenin-mediated transcription

Dan-Qian Chen*, Xia-Qing Wu*, Lin Chen, He-He Hu, Yan-Ni Wang and Ying-Yong Zhao

Abstract

Background: Renal fibrosis is the common feature of chronic kidney disease (CKD). However, few drugs specifically target fibrogenesis due to the lack of an effective therapeutic target. Hence, it is urgent to find a therapeutic strategy that inhibits renal fibrosis. Here, we identified that poricoic acid A (PAA) as the modulator of tryptophan hydroxylase-1 (TPH-1), the key enzyme in tryptophan metabolism, exerted potent anti-fibrotic effects in the kidney.

Methods: Lentiviral vector, luciferase reporter activity assay and co-immunoprecipitation were used. The animal model of unilateral ureteral obstruction and adenine-induced chronic renal failure as well as transforming growth factor (TGF)-β1-treated epithelial cells NRK-52E and fibroblasts NRK-49F were used.

Results: TPH-1 was gradually decreased during CKD progression, while PAA treatment significantly increased TPH-1 expression to suppress renal fibrosis. Pharmacological overexpression of TPH-1 by PAA treatment exhibited anti-fibrosis and was linked to Wnt/β-catenin signaling activity. TPH-1 exhibited anti-fibrotic effects by suppressing epithelial cell injury and fibroblast activation, and PAA promoted TPH-1 expression and then suppressed the Wnt/β-catenin signaling pathway *via* regulating the protein stability of β-catenin and β-catenin-mediated transcription. TPH-1 overexpression enhanced the anti-fibrotic effects of PAA, while TPH-1 deficiency weakened the anti-fibrotic effects of PAA, indicating that TPH-1 was required for the anti-fibrotic effects of PAA.

Conclusion: PAA as a modulator of TPH-1 expression attenuated renal fibrosis through regulating the Wnt/β-catenin signaling pathway by acting on the protein stability of β-catenin and β-catenin-mediated transcription. TPH-1 was required for PAA to exert anti-fibrosis.

Keywords: chronic kidney disease, fibroblast, poricoic acid A, TPH-1, renal fibrosis, Wnt/β-catenin

Received: 24 May 2020; revised manuscript accepted: 9 September 2020.

Correspondence to:
Ying-Yong Zhao
Faculty of Life Science and Medicine, Northwest University, No. 229 Taibai North Road, Xi'an, Shaanxi 710069, China
zyy@nwu.edu.cn

Dan-Qian Chen
Faculty of Life Science and Medicine, Northwest University, Xi'an, Shaanxi, China

Beijing Key Lab for Immune-mediated Inflammatory Diseases, Department of Pharmacology, Institute of Clinical Medical Sciences, China-Japan Friendship Hospital, Beijing, China

Xia-Qing Wu
Lin Chen
He-He Hu
Yan-Ni Wang
Faculty of Life Science and Medicine, Northwest University, Xi'an, Shaanxi, China

*These authors contributed equally

Introduction

Chronic kidney disease (CKD) has affected more than 10% of people worldwide and increased the risk of cardiovascular disease, diabetes and even cancer.[1,2] The prevalence of CKD and its economic burden continues to increase.[2] Failure to treat CKD effectively contributes to the progression to end-stage renal disease that needs dialysis or transplantation. Fibrosis, the common feature of various CKDs, is characterized as the replacement of normal tissue by scar tissue, and finally causes declined kidney function.[3] The blockage of fibrogenesis is beneficial to CKD treatment. However, few medicines in clinical medicine directly target fibrogenesis.[4] It is well known that transforming growth factor (TGF)-β1 inhibition is effective to attenuate fibrosis, but the constraints involved in the pleiotropic effects of

TGF-β1, such as its immune suppressive and anti-proliferative effects, hinder drug research and development.[5,6] Hence, it is urgent to discover medication that not only effectively attenuates renal fibrosis and also needs to be safe.

Natural products have recently become increasingly recognized as alternative sources for ameliorating renal fibrosis. *Poria cocos* is commonly used as a food or medicine to treat renal fibrosis in Asia.[7] Tetracyclic triterpenoids isolated form *P. cocos* exhibited good therapeutic effects against renal fibrosis.[8,9] Poricoic acid A (PAA) is the main component of *P. cocos* and showed inhibitory effects on renal fibrosis in several animal and cell models.[10–12] Here, we found that PAA could modulate tryptophan hydroxylase-1 (TPH-1),[8] a novel therapeutic target for renal fibrosis, to exert its renoprotection.

TPH-1 is the key enzyme in the synthesis from *L*-tryptophan to 5-methoxytryptophan (5-MTP), which exhibits protective effects in cardiomyocytes against hydrogen peroxide (H_2O_2)-induced oxidative injury, post-myocardial infarction and ventricular remodeling.[13–15] Importantly, our latest studies found that CKD led to the decrease in serum 5-MTP levels,[16] and further studies found that TPH-1 promoted 5-MTP expression that ameliorated inflammation in the kidney *via* inhibiting IκB/NF-κB signaling and activating Keap1/Nrf2 signaling.[16] These results confirmed the anti-inflammatory effects of TPH-1 and indicated that TPH-1 had the potential to be developed as a therapeutic target for treating CKD. However, the mechanism of anti-fibrotic and renoprotective effects of TPH-1 remained obscure. Here, we not only found that PAA could promote TPH-1 expression to attenuate renal fibrosis, and also proved the mechanisms underlying the anti-fibrotic and renoprotective effects of TPH-1.

The Wnt/β-catenin signaling pathway plays a key role in mediating renal fibrosis and CKD progression.[17–19] The Wnt/β-catenin signaling pathway is silent in normal adult kidney, but activates once an injury occurs.[20,21] The activation of the Wnt/β-catenin signaling pathway resulted in renal epithelial cell injury and fibroblast activation thus causing extracellular matrix (ECM) accumulation.[5,22] β-Catenin plays the central role in this signaling pathway.[23,24] In the absence of Wnt ligands, β-catenin normally maintains at a low level in the cytoplasm due to its association with a destruction complex including Axin1 and glycogen synthase kinase 3β (GSK-3β). Axin1 is the scaffold protein of this complex, while GSK-3β phosphorylates β-catenin, thus leading to its ubiquitin-dependent degradation.[23,24] Upon stimulation by Wnt ligands, β-catenin protein stabilizes and accumulates in the cytoplasm and then transfers in the nucleus, where it binds to T-cell factor/lymphoid enhancer factor (TCF/LEF) transcription factors, initiating the expression of downstream target genes that promote renal fibrosis.[5,17] Therefore, the inhibition of the Wnt/β-catenin signaling pathway is beneficial for anti-fibrosis and CKD treatment.

In the present study, we identified PAA as a modulator of TPH-1 to exert anti-fibrotic and renoprotective effects *via* regulating the Wnt/β-catenin signaling pathway. Firstly, we demonstrated the gradual downregulation of TPH-1 during CKD progression, and PAA treatment could promote TPH-1 expression to attenuate renal fibrosis. Then, we investigated the role of TPH-1 in renal fibrosis, and found that TPH-1 exerted protective effects on CKD and had the potential to be developed as the therapeutic target for treating renal fibrosis through modulating the Wnt/β-catenin signaling pathway by acting on the protein stability of β-catenin and β-catenin-mediated transcription.

Methods

Animal treatment

This part of the animal study was carried out in strict accordance with the recommendations in the Guide for the Care and Use of Laboratory Animals of the State Committee of Science and Technology of the People's Republic of China, and the protocol was approved by the Committee on the Ethics of Animal Experiments of the Northwest University (permit number: SYXK 2010-004). All surgery was performed under anesthesia, and all efforts were made to minimize suffering. All procedures and care of the rats were in accordance with the institutional guidelines for animal use in research. Male BALB/c mice, weighing 20–22 g, were purchased from the Animal Centre of Xi'an Jiaotong University (Xi'an, Shaanxi) and used to establish a unilateral ureteral obstruction (UUO) and adenine-induced chronic renal failure (CRF) model. Mice were

provided with food and water and housed in plastic cages (≤5 mice per cage) with 40–70% humidity at 22 ± 2°C and 12 h light/12 h dark cycle. Mice were acclimatized to their housing environment for 7 days before experimentation and to the experimental room for 1 h before experiments. Animal studies in the present study are reported in compliance with the ARRIVE guidelines.

After general anesthesia with sodium pentobarbital by intraperitoneal injection (1%, 50 mg/kg), complete UUO was carried out through double-ligating the left ureter by 4–0 silk after the dorsal incision. The ureters of sham-operated mice were only exposed, but not ligated. Adenine-induced CRF mice were administered 0.2% adenine-containing diet for 3 weeks, while control mice were administered normal diet. PAA was given to mice at the dose of 10 mg/kg by intragastric administration each day, while ICG-001 (Selleck Chemicals, USA), the inhibitor of the Wnt/β-catenin signaling pathway, was intraperitoneally injected at the dose of 5 mg/kg each day. In addition, the extraction and isolation of PAA were consistent with a previous study.[10] Mice were sacrificed at the 1st, 2nd and 3rd weeks, respectively. The ligated and adenine-treated kidneys were immediately frozen and stored in liquid nitrogen for following experiments.

Cell culture and treatment

Normal renal kidney epithelial cells (NRK-52E) and normal renal kidney fibroblasts (NRK-49F) were purchased from the China Center for Type Culture Collection. NRK-52E and NRK-49F were cultured in dulbeccos's modified eagle's mediucm/F-12 supplemented with 10% fetal bovine serum at 37°C with 5% carbon dioxide. NRK-52E and NRK-49F cells were treated with 2.5 ng/mL and 5.0 ng/mL recombinant human TGF-β1 protein (R&D Systems, USA) respectively. The concentrations of PAA for NRK-52E and NRK-49F cells were 10 μM. After 24 h of treatment, cells were harvested for following experiments.

Knock-in and knock-down of TPH-1 or TCF4

Lentivirus expressing full-length *Tph1* cDNA (TPH-1 over), lentivirus containing empty plasmids (vector), lentivirus expressing shRNA against *Tph1* (TPH-1 shRNA), lentivirus containing scramble (scramble), lentivirus expressing full-length rat *Tcf4* cDNA (TCF4 over) and lentivirus expressing shRNA against rat *Tcf4* (TCF4 shRNA) were constructed by Sangon Biotech Company (Shanghai, China). For *in vitro* study, NRK-52E and NRK-49F cells were seeded in the 6-well plate until they reached 70–80% confluence. The transfection complex was directly added to the medium, and the medium was removed after 24 h. The final titers of the lentiviral vector were determined to contain 1×10^8 TU/mL. For *in vivo* study, after anesthesia and dorsal incision, mice were injected with saline or recombinant lentivirus vector by a 31 G needle at the lower pole of the kidney parallel to the long axis. The 100 μL of saline or lentivirus cocktail (1×10^5 IU/μL) were injected into the kidney.

Masson's trichrome staining

Kidney tissues were collected and fixed by 4% paraformaldehyde for 24 h, then were embedded in paraffin and made into serial sections with 5 μm of thickness for Masson's trichrome staining. Masson's trichrome staining for kidney tissues was carried out as described previously.[25,26]

Immunohistochemical staining

Paraffin-embedded mouse kidney sections were prepared as a routine procedure. Immunohistochemical staining for kidney tissues was carried out as described previously.[27] Briefly, slides of 5 μm thickness were pretreated with citrate buffer (10 mM sodium citrate, pH 6.0) for heat-induced epitope retrieval, and then blocked with 3% H_2O_2 to clean endogenous peroxidase. After that, slides were incubated with 10% goat serum for 1 h to block non-specific sites. Primary antibodies were incubated at 4°C overnight, and secondary antibodies were incubated at room temperature for 1 h. Slides were developed by 3,3-*N*-diaminobenzidine tertrahydrochloride and counterstained with Harris hematoxylin. The slides were mounted on neutral gum. Image analysis was done by using Image-Pro Plus 6.0 software. To show these results better, the value of protein expression in control (CTL) or the sham-operated group was further normalized to 1 by using the mean.

Immunofluorescence staining and confocal microscopy

Briefly NRK-52E and NRK-49F cells cultured on coverslips were fixed with 4% paraformaldehyde

for 10 min, and 10% goat serum was used to block non-specific sites. The slides were incubated with primary antibodies at 4°C overnight, incubated with secondary antibodies at room temperature for 2 h and incubated with propidium iodide for 10 min, respectively. Then the slides were mounted with 80% glycerinum in phosphate buffered saline (PBS), and examined by a laser-scanning confocal microscope (FV1000, Olympus, Japan) equipped with a FV10-ASW 4.2 viewer (Olympus, Japan). To show these results better, the value of protein expression in CTL or the sham-operated group was further normalized to 1 by using the mean.

Western blot analysis

Protein expression was analyzed by western blot analysis. Cells or kidney tissues were lysed by using M-PER mammalian protein extraction reagent (78501, Thermo Scientific, USA) and protein concentration was measured by using BCA protein assay kit (23227, Thermo Scientific, USA). Nuclear protein was extracted by using NE-PER nuclear and cytoplasmic extraction reagents (78835, Thermo Scientific, USA). The 20–30 μg of total protein was fractionated by tris-glycine resolving gel and then transferred to a 0.45 μm polyvinylidene difluoride (PVDF) membrane (10600023, GE Healthcare, USA). PVDF membranes were incubated in 5% non-fat milk-blocking buffer for 1 h to block non-specific sites. PVDF membranes were incubated at 4°C in primary antibody overnight, and incubated in secondary antibodies of goat anti-rabbit (1:5000, ab6721; Abcam, USA) or goat anti-mouse (1:5000, A21010; Abbkine, USA) for 2 h at room temperature. PVDF membranes were then visualized by enhanced chemiluminescence western blotting detection reagent, and signal intensities of immunoblots were quantified by using Image J software (version 1.48v; NIH, USA). Band densities were normalized by α-tubulin or histone H3 expression levels. To show these results better, the value of protein expression in CTL or the sham-operated group was further normalized to 1 by using the mean.

The following primary antibodies were employed: TPH-1 (1:500, ab52954; Abcam, USA), ubiquitin (1:1000, sc-166553; Santa Cruz Biotechnology, USA), collagen I (1:5000, ab34710; Abcam, USA), alpha smooth muscle actin (α-SMA, 1:500, ab7817; Abcam, USA), fibronectin (1:1000, ab2413; Abcam, USA), E-cadherin (1:500, ab76055; Abcam, USA), β-catenin (1:1000, 610154; BD Transduction Laboratories, USA), snail1 (1:1000, ab180714; Abcam, USA), twist (1:2000, ab50581; Abcam, USA), matrix metallopeptidase-7 (MMP-7, 1:400, ab5706; Abcam, USA), plasminogen activator inhibitor-1 (PAI-1, 1;5000, 612024; BD Transduction Laboratories, USA), GSK-3β (1:2000, 9315; Cell Signaling Technology, USA), Axin1 (1:2000, 3323; Cell Signaling Technology, USA) and TCF4 (1:2000, 2565; Cell Signaling Technology, USA). α-Tubulin and histone H3 were purchased from Proteintech Company (Hubei, China).

Co-immunoprecipitation (Co-IP)

Cells or kidney tissues were washed in PBS and lysed with lysis buffer (78501; Thermo Scientific, USA), and then lysates were pretreated with protein A/G (Immunoprecipitation Starter Pack; GE Healthcare, USA) for 1 h at 4°C to avoid any interference caused by antibodies presented in the cell lysates. The supernatant was incubated with anti-ubiquitin (1:100), anti-β-catenin (1:100) and anti-TCF4 (1:100) antibodies overnight at 4°C to couple antigen with antibody, and then was immune-precipitated by protein A/G overnight at 4°C to precipitate the immune complexes. The complexes were washed six times with cell lysis buffer. Both the input and co-IP samples were analyzed by western blot analysis as described above.

TCF/LEF reporter assay

The Cignal TCF/LEF reporter assay kit (336841; Qiagen, USA) was used to quantify the specific activation of β-catenin-dependent Wnt signaling according to the manufacturer's protocol. Briefly, NRK-52E and NRK-49F cells were seeded in the 96-well plate and treated as indicated. Vectors were transfected by Lipofectamine 3000 (Invitrogen, USA) with a final volume of 200 μL. After culturing for 24–48 h duration, the medium was removed. Then, the firefly fluorescence and the renilla fluorescence were measured by using dual-luciferase reporter assay system (E1910; Promega, USA) according to the manufacturer's protocol.

Statistics

The number of replicates was six per group for each data set. The results were presented as

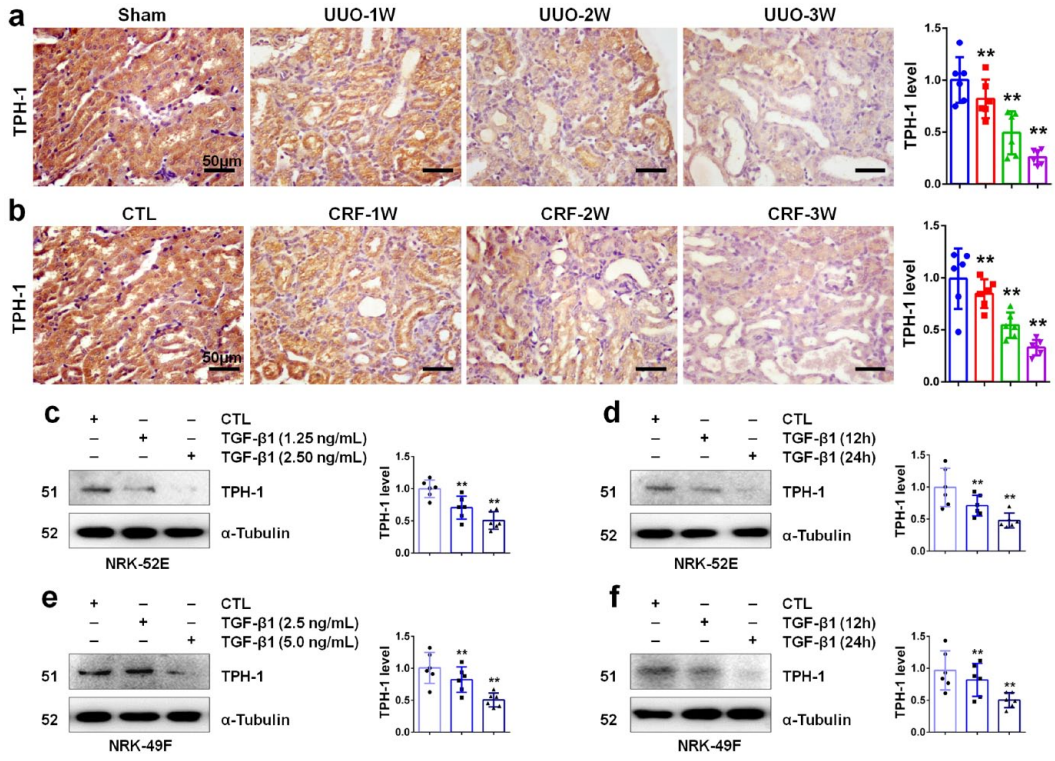

Figure 1. TPH-1 was impaired in CKD. (a) Immunohistochemical staining of TPH-1 in UUO mice. (b) Immunohistochemical staining of TPH-1 in CRF mice. Blue, sham or CTL group; red, UUO or CRF group at 1st week after surgery; green, UUO or CRF group at 2nd week after surgery; purple, UUO or CRF group at 3rd week after surgery. (c) The protein expression and relative quantitative data of TPH-1 in NRK-52E cells after 24 h stimulation. (d) The protein expression and relative quantitative data of TPH-1 in NRK-52E cells at a dose of 2.5 ng/mL. (e) The protein expression and relative quantitative data of TPH-1 in NRK-49F cells after 24 h stimulation. (f) The protein expression and relative quantitative data of TPH-1 in NRK-49F cells at a dose of 5.0 ng/mL. Light purple, CTL group; blue and gray-black, TGF-β1-treated group.
$^{**}p < 0.01$ compared with sham-operated or CTL group ($n = 6$).
Dot presented the single data results in the bar graph.
CKD, chronic kidney disease; CRF, chronic renal failure; CTL, control; TGF, transforming growth factor; TPH-1, tryptophan hydroxylase-1; UUO, unilateral ureteral obstruction.

mean ± standard deviation unless stated otherwise. GraphPad Prism software version 6.0 (San Diego, CA, USA) was used for statistical analysis. Statistical analysis for multiple groups was performed by one-way analysis of variance followed by Dunnett's *post hoc* test when F achieved $p < 0.05$ and there was no significant variance in homogeneity. Some results were normalized to control to avoid unwanted sources of variation. $p < 0.05$ was considered statistically significant.

Results

TPH-1 was downregulated in progressive CKD

We first investigated the expression of TPH-1 during progressive CKD by using a UUO and adenine-induced CRF mouse model. UUO is a common model for studying tubulo-interstitial fibrosis (TIF). As shown in Figure 1a, UUO resulted in the gradual downregulation of TPH-1 protein in a time-dependent manner in obstructed kidney tissues of BALB/c mice. The adenine-induced CRF model, the non-surgical method for induction of CKD in mice, is used to investigate toxicant-induced TIF.[28] Oral administration of adenine induced the reduction of TPH-1 in a protein time-dependent manner in kidney tissues (Figure 1b). Next, we examined the TPH-1 expression in renal epithelial cells and fibroblasts. As shown in Figure 1c, TGF-β1 suppressed TPH-1 expression, and stimulation with a 2.5 ng/mL dose of TGF-β1 performed stronger inhibitory effects than with a 1.25 ng/mL dose. As shown in Figure

1d, stimulation with TGF-β1 for 24h showed stronger inhibitory effects than for 12h in NRK-52E cells. These results indicated TGF-β1 stimulation declined TPH-1 expression in a dose and time-dependent manner in NRK-52E cells, which was consistent with those in NRK-49F cells in Figure 1e, f. These results indicated the gradual downregulation of TPH-1 in progressive CKD.

PAA served as a modulator of TPH-1 expression to attenuate renal fibrosis

Epithelial–mesenchymal transition (EMT) and ECM accumulation are important features of fibrosis, accompanied by the increase in collagen I, fibronectin, α-SMA and the decrease in E-cadherin.[29,30] We investigated the regulatory role of PAA on TPH-1 expression in mouse models of UUO and CRF. As shown in Figure 2a and b, both UUO and adenine resulted in the downregulation of TPH-1 expression, while PAA treatment rescued TPH-1 expression in kidney tissues, accompanied by decreased collagen I, fibronectin, α-SMA expression and increased E-cadherin expression. These results indicated that PAA inhibited ECM accumulation and EMT through increasing TPH-1 expression. Similar results were also observed in NRK-52E and NRK-49F cells. As shown in Figure 2c and d, in the absence of TGF-β1, PAA treatment slightly increased TPH-1 expression, but did not reach statistical significance. TGF-β1 stimulation significantly declined TPH-1 expression, while PAA treatment rescued TPH-1 expression in NRK-52E and NRK-49F cells, accompanied by increased E-cadherin and decreased α-SMA expression, respectively. We next examined the luciferase activity of TCF/LEF reporter. As shown in Figure 2e, PAA could inhibit TGF-β1-induced luciferase activity of TCF/LEF reporter. These results demonstrated that PAA inhibited epithelial cell injury and fibroblast activation through increasing TPH-1 expression, which may be associated with the Wnt/β-catenin signaling pathway.

TPH-1 ameliorated renal fibrosis through inhibiting epithelial cell injury and fibroblast activation

Although we have demonstrated that PAA increased TPH-1 expression to inhibit renal fibrosis, the role of TPH-1 in renal fibrosis remains unclear. To decipher the role of TPH-1, lentivirus expressing shRNA against *Tph1* and lentivirus expressing full-length *Tph1* cDNA were employed and indicated in Supplemental Figure 1. Lentivirus expressing shRNA against *Tph1* significantly decreased TPH-1 expression, while lentivirus expressing full-length *Tph1* cDNA significantly increased TPH-1 expression. As shown in Figure 3a and b, both UUO and adenine mediated the upregulation of collagen I, fibronectin, α-SMA and the downregulation of the epithelial cell marker E-cadherin expression in kidney tissues. After knock-down of TPH-1, these abnormalities exacerbated, which indicated the anti-fibrotic effects of TPH-1. As shown in Figure 3c and d, TGF-β1 caused the downregulation of E-cadherin expression in NRK-52E cells and the upregulation of the myofibroblast marker α-SMA expression in NRK-49F cells, indicating injured epithelial cells and activated fibroblasts. TPH-1 deficiency contributed to TGF-β1-induced downregulation of E-cadherin and upregulation of α-SMA, while TPH-1 overexpression inhibited these abnormalities, which confirmed the protective role of TPH-1 in renal fibrosis. These results pointed out that TPH-1 deficiency exacerbated renal fibrosis, while TPH-1 overexpression inhibited renal fibrosis through suppressing epithelial cell injury and fibroblast activation.

TPH-1 suppressed Wnt/β-catenin signaling activation

Although we demonstrated the anti-fibrotic and renoprotective effects of TPH-1, its underlying mechanisms remained obscure. Due to the importance of the Wnt/β-catenin signaling pathway in renal fibrosis and the regulatory role of PAA on the Wnt/β-catenin signaling pathway in Figure 2e, we next tested whether TPH-1 functionally regulated the Wnt/β-catenin signaling pathway. As shown in Figure 4a, TGF-β1 induced luciferase activity of TCF/LEF reporter in NRK-52E and NRK-49F cells, while luciferase activity significantly increased after knock-down of TPH-1. Notably, luciferase activity significantly decreased after knock-in of TPH-1, which was consistent with those results after PAA treatment in Figure 2e. These results pointed to TPH-1 overexpression by PAA treatment suppressed Wnt/β-catenin activity. Further studies investigated the expression of β-catenin protein, the pivotal molecule in this signaling. As shown in Figure 4b, TGF-β1

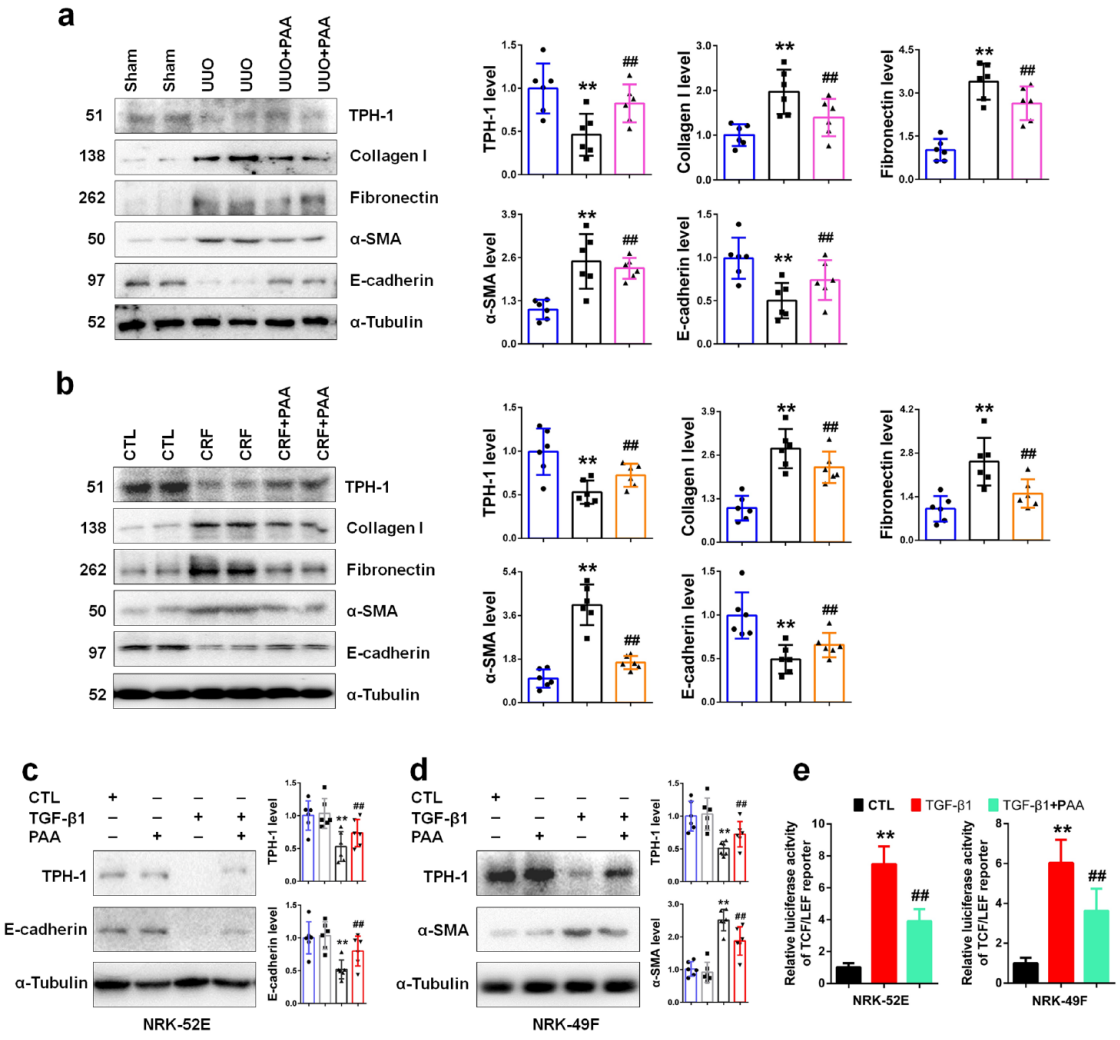

Figure 2. PAA promoted TPH-1 expression to suppress renal fibrosis. (a) The protein expression and relative quantitative data of TPH-1, collagen I, fibronectin, α-SMA and E-cadherin in UUO mice. (b) The protein expression and relative quantitative data of TPH-1, collagen I, fibronectin, α-SMA and E-cadherin in CRF mice. Blue, sham or CTL group; gray-black, UUO or CRF group; pink or orange, UUO + PAA or CRF + PAA group. (c) The protein expression and relative quantitative data of TPH-1 and E-cadherin in NRK-52E cells. (d) The protein expression and relative quantitative data of TPH-1 and α-SMA in NRK-49F cells. Blue, CTL group; gray, PAA-treated group; black, TGF-β1-treated group; red, TGF-β1 + PAA group. (e) The luciferase activity of TCF/LEF reporter in NRK-52E and NRK-49F cells.

$^{**}p < 0.01$ compared with sham-operated or CTL group ($n = 6$).

$^{\#\#}p < 0.01$ compared with UUO, CRF or TGF-β1-treated group ($n = 6$).

Dot presented the single data results in the bar graph.

CRF, chronic renal failure; CTL, control; PAA, poricoic acid A; α-SMA, alpha smooth muscle actin; TCF/LEF, T-cell factor/lymphoid enhancer factor; TGF, transforming growth factor; TPH-1, tryptophan hydroxylase-1; UUO, unilateral ureteral obstruction.

stimulation promoted β-catenin expression in the nucleus in both NRK-52E and NRK-49F cells. After knock-down of TPH-1, β-catenin expression was significantly increased in the nucleus in NRK-52E and NRK-49F cells. TPH-1 overexpression resulted in the downregulation of β-catenin protein in the nucleus (Figure 4c). These results indicated the inhibition of TPH-1 on β-catenin expression in the nucleus. We further examined the expression of downstream target genes of the Wnt/β-catenin signaling pathway. As shown in Figure 4d, TGF-β1 stimulation increased the protein expression of downstream target genes of the Wnt/β-catenin signaling pathway, including twist, snail1, MMP-7 and PAI-1, while TPH-1 overexpression inhibited the upregulation of these

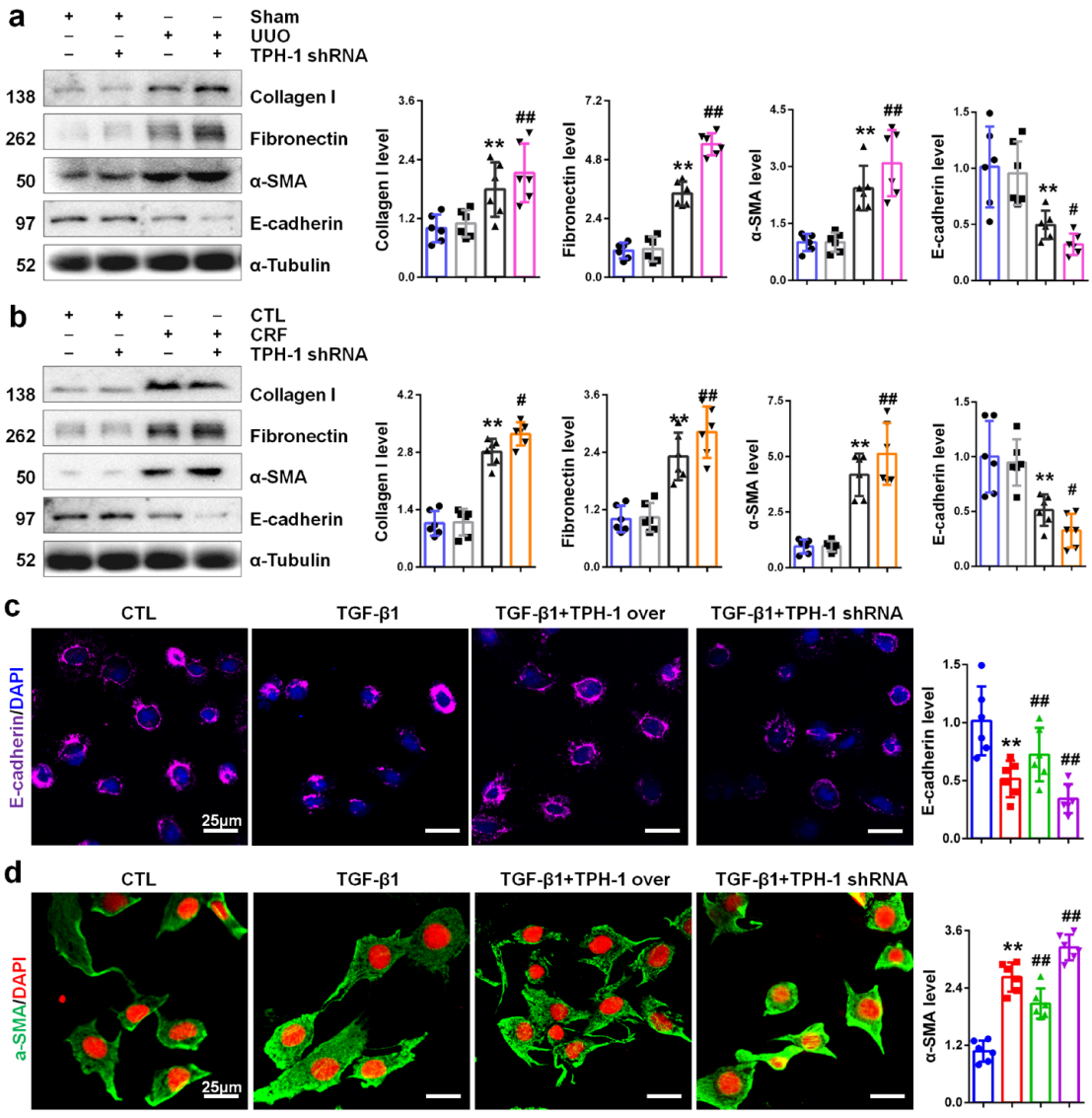

Figure 3. TPH-1 suppressed renal damage and fibrosis. (a) The protein expression and relative quantitative data of collagen I, fibronectin, α-SMA and E-cadherin in UUO mice. (b) The protein expression and relative quantitative data of collagen I, fibronectin, α-SMA and E-cadherin in CRF mice. Blue, sham or CTL group; gray, TPH-1 shRNA-transfected group; black, UUO or CRF group; pink or orange, UUO + TPH-1 shRNA or CRF + TPH-1 shRNA group. (c) Immunofluorescence staining of E-cadherin in NRK-52E cells. (d) Immunofluorescence staining of α-SMA in NRK-49F cells. Blue, CTL group; red, TGF-β1-treated group; green, TGF-β1 + TPH-1 over group; purple, TGF-β1 + TPH-1 shRNA group.
$^{**}p < 0.01$ compared with sham-operated or CTL group ($n = 6$).
$^{\#\#}p < 0.01$ compared with UUO, CRF or TGF-β1-treated group ($n = 6$).
Dot presented the single data results in the bar graph.
CRF, chronic renal failure; CTL, control; PAA, poricoic acid A; α-SMA, alpha smooth muscle actin; TGF, transforming growth factor; TPH-1, tryptophan hydroxylase-1; UUO, unilateral ureteral obstruction.

downstream target genes in NRK-52E cells. Similar results were also observed in NRK-49F cells (Supplemental Figure 2). These results demonstrated that TPH-1 negatively regulated the expression of β-catenin protein.

We next investigated whether TPH-1 played a role in mediating Wnt/β-catenin-mediated fibrosis. As TCF4 serves as the transcriptional partner of β-catenin,[23] lentivirus expressing shRNA against rat *Tcf4* and lentivirus expressing full-length rat *Tcf4*

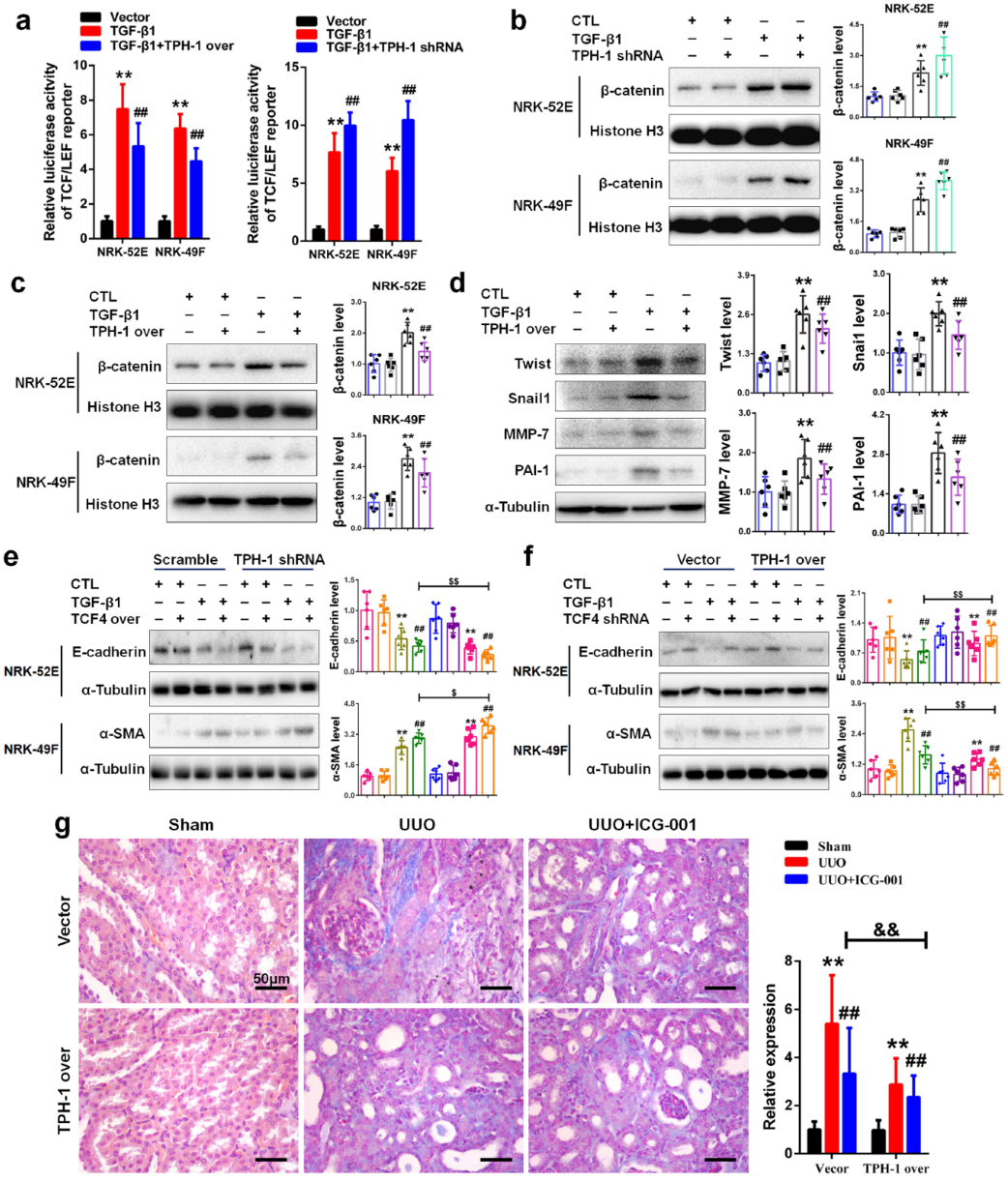

Figure 4. TPH-1 inhibited the activation of Wnt/β-catenin signaling. (a) The luciferase activity of TCF/LEF reporter in NRK-52E and NRK-49F cells. (b) The protein expression and relative quantitative data of β-catenin in the nucleus of NRK-52E and NRK-49F cells. (c) The protein expression and relative quantitative data of β-catenin in the nucleus of NRK-52E and NRK-49F cells. (d) The protein expression and relative quantitative data of twist, snail1, MMP-7 and PAI-1 in NRK-52E cells. Blue, CTL group; gray, TPH-1 shRNA or TPH-1 over group; black, TGF-β1-treated group; bright green or purple, TGF-β1 + TPH-1 shRNA or TGF-β1 + TPH-1 over group. (e) The protein expression and relative quantitative data of E-cadherin and α-SMA in NRK-52E and NRK-49F cells, respectively. (f) The protein expression and relative quantitative data of E-cadherin and α-SMA in NRK-52E and NRK-49F cells, respectively. (g) Masson's trichrome staining of kidney tissues of UUO mice.

$^{**}p < 0.01$ compared with sham-operated or CTL group ($n = 6$).

$^{\#\#}p < 0.01$ compared with UUO or TGF-β1-treated group ($n = 6$).

$^{\$}p < 0.05$.

$^{\$\$}p < 0.01$ compared with TGF-β1 + TCF4 shRNA or TGF-β1 + TCF4 over group after transfected with vector or scramble ($n = 6$).

$^{\&\&}p < 0.01$ compared with UUO + ICG-001 group.

Dot presented the single data results in the bar graph.

CTL, control; MMP-7, matrix matallopeptidase-7; PAI-1: plasminogen activator inhibitor-1, α-SMA, alpha smooth muscle actin; TCF/LEF, T-cell factor/lymphoid enhancer factor; TGF, transforming growth factor; TPH-1, tryptophan hydroxylase-1; UUO, unilateral ureteral obstruction.

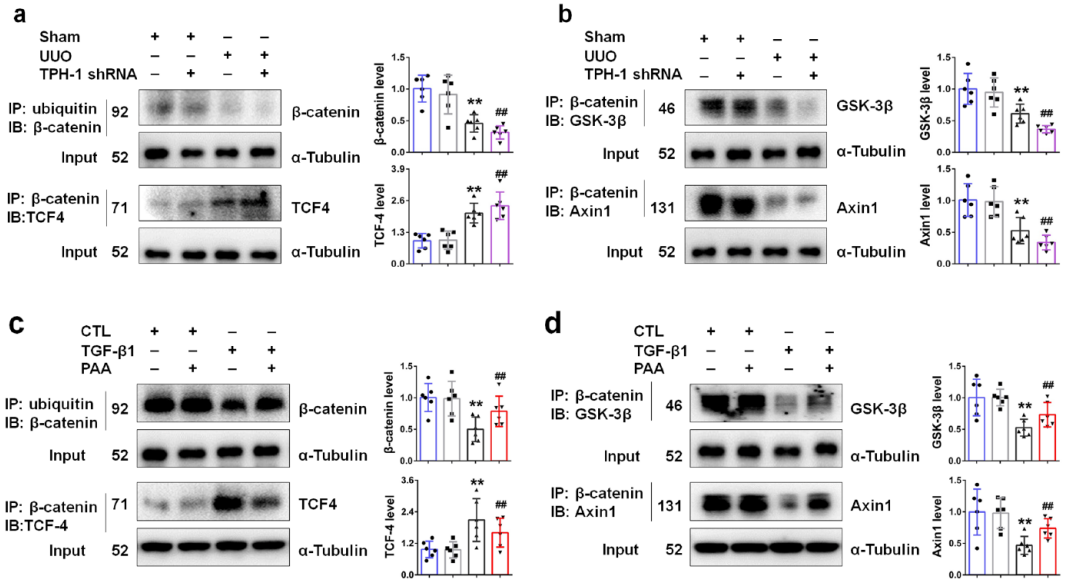

Figure 5. PAA promoted TPH-1 expression to regulate the protein stability of β-catenin and β-catenin-mediated transcription. (a) The protein expression and relative quantitative data of β-catenin and TCF4 in UUO mice. (b) The protein expression and relative quantitative data of GSK-3β and Axin1 in UUO mice. (c) The protein expression and relative quantitative data of β-catenin and TCF4 in NRK-52E cells. (d) The protein expression and relative quantitative data of GSK-3β and Axin1 in NRK-52E cells. Blue, sham or CTL group; gray, TPH-1 shRNA-transfected or PAA-treated group; black, UUO or TGF-β1-treated group; purple or red, UUO + TPH-1 shRNA or TGF-β1 + PAA group.
$^{**}p < 0.01$ compared with sham-operated or CTL group ($n = 6$).
$^{\#\#}p < 0.01$ compared with UUO or TGF-β1-treated group ($n = 6$).
Dot presented the single data results in the bar graph.
CTL, control; GSK, glycogen synthase kinase 3β; PAA, poricoic acid A; TGF, transforming growth factor; TPH-1, tryptophan hydroxylase-1; UUO, unilateral ureteral obstruction.

cDNA were used. As indicated in Supplemental Figure 3, lentivirus expressing shRNA against *Tcf4* significantly decreased TCF4 expression, while lentivirus expressing full-length *Tcf4* cDNA significantly increased TCF4 expression. Firstly, as shown in Figure 4e, TCF4 overexpression contributed to TGF-β1-induced downregulation of E-cadherin, and simultaneously, TPH-1 deficiency exacerbated epithelial cell injury indicated by increased loss of E-cadherin. Similar results were also observed in NRK-49F cells. Overexpression of TCF4 in NRK-49F cells increased α-SMA expression, and these effects could be enhanced in TPH-1-silenced cells. Secondly, as shown in Figure 4f, TCF4 deficiency inhibited fibrosis, but not as significantly as those under TPH-1 overexpression. Then, ICG-001, the inhibitor of Wnt/β-catenin signaling, was employed to illuminate the effects of TPH-1 against Wnt/β-catenin activity *in vivo*. As shown in Figure 4g, compared with the vector-transfected group, TPH-1 overexpression enhanced the effects of ICG-001 in UUO-induced renal fibrosis. Taken together, our results indicated the inhibition of TPH-1 on Wnt/β-catenin signaling activity.

PAA promoted TPH-1 expression to regulate the protein stability of β-catenin and β-catenin-mediated transcription

To decipher better the molecular mechanism of TPH-1 in modulating Wnt/β-catenin signaling, we began our study by exploring the interaction within Wnt/β-catenin signaling. As shown in Figure 5a, UUO inhibited the interaction of ubiquitin and β-catenin, pointing to the inhibited ubiquitin-dependent degradation of β-catenin protein in obstructed kidney tissues. UUO also promoted the interaction of β-catenin and TCF4, pointing to enhanced transcription mediated by β-catenin in obstructed kidney tissues. Notably, TPH-1 deficiency exacerbated these abnormal changes. We further explored the deep mechanisms underlying the ubiquitin-dependent degradation of β-catenin protein. The ubiquitin-dependent degradation of β-catenin protein is mediated by the cytoplasmic destruction

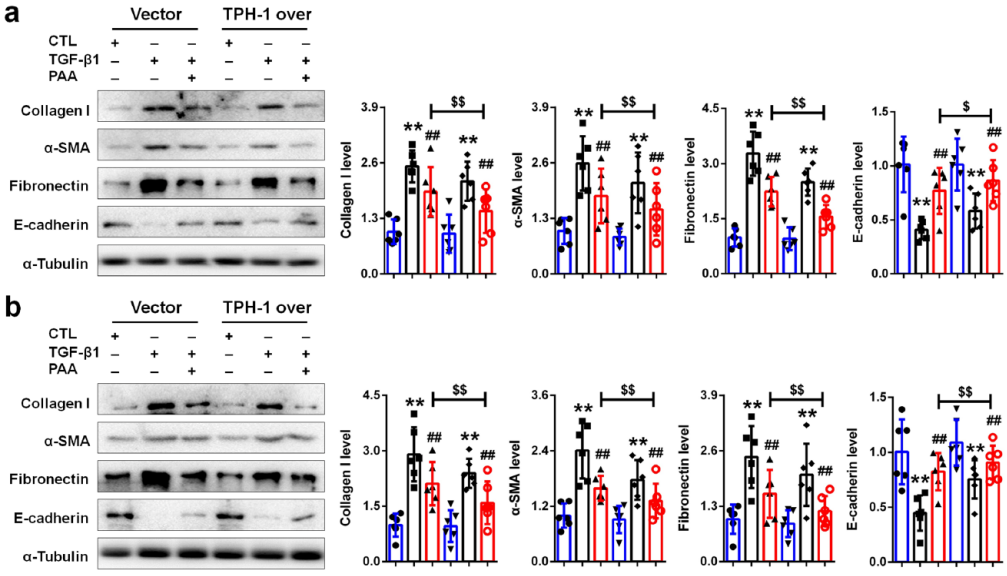

Figure 6. TPH-1 overexpression enhanced anti-fibrotic effects of PAA. (a) The protein expression and relative quantitative data of collagen I, α-SMA, fibronectin and E-cadherin in NRK-52E cells. (b) The protein expression and relative quantitative data of collagen I, α-SMA, fibronectin and E-cadherin in NRK-49F cells. Blue, CTL group; black, TGF-β1-treated group; red, TGF-β1 + PAA group.
$^{**}p < 0.01$ compared with CTL group ($n = 6$).
$^{\#\#}p < 0.01$ compared with TGF-β1-treated group ($n = 6$).
$^{\$}p < 0.05$.
$^{\$\$}p < 0.01$ compared with TGF-β1 + PAA group after transfected with vector ($n = 6$).
Dot presented the single data results in the bar graph.
CTL, control; PAA, poricoic acid A; α-SMA, alpha smooth muscle actin; TGF, transforming growth factor; TPH-1, tryptophan hydroxylase-1.

complex. Within the destruction complex, Axin1 serves as the scaffold protein, while GSK-3β is vital in β-catenin phosphorylation and thereby ubiquitin-dependent degradation.[24] As shown in Figure 5b, UUO inhibited the interaction of β-catenin with GSK-3β and Axin1 in obstructed kidney tissues, which indicated the stability of β-catenin protein. However, after knock-down of TPH-1, the interaction of β-catenin with GSK-3β and Axin1 became weaker, indicating the inhibited ubiquitin-dependent degradation of β-catenin protein. These results demonstrated that TPH-1 modulated the stability of β-catenin protein and β-catenin-mediated transcription. Taken together, TPH-1 had the potential to be developed as a therapeutic target and exerted its anti-fibrotic effects through modulating Wnt/β-catenin signaling activity.

To clarify the underlying mechanisms of PAA in modulating TPH-1 expression and Wnt/β-catenin signaling activity, co-IP analysis was employed. As shown in Figure 5c, TGF-β1 inhibited the interaction of ubiquitin and β-catenin, which suppressed the degradation of β-catenin protein, while PAA treatment contributed to the interaction of ubiquitin and β-catenin to promote the degradation of β-catenin protein. Simultaneously, TGF-β1-induced separation of β-catenin with GSK-3β and Axin1 were inhibited after PAA treatment (Figure 5d). In addition, PAA treatment also suppressed the interaction of β-catenin and TCF4 (Figure 5c). The effect of PAA treatment was similar to the effect of TPH-1 overexpression and PAA could increase TPH-1 expression, which indicated PAA effects involved in TPH-1 overexpression. Taken together, PAA increased TPH-1 expression and further suppressed Wnt/β-catenin signaling activity to attenuate renal fibrosis through inhibiting the protein stability of β-catenin and β-catenin-mediated transcription.

TPH-1 was required for PAA to exert anti-renal fibrosis

To clarify whether TPH-1 was required for PAA to exert its anti-renal fibrosis, lentivirus expressing full-length rat *Tph1* cDNA was employed. As shown in Figure 6a and b, TPH-1 overexpression

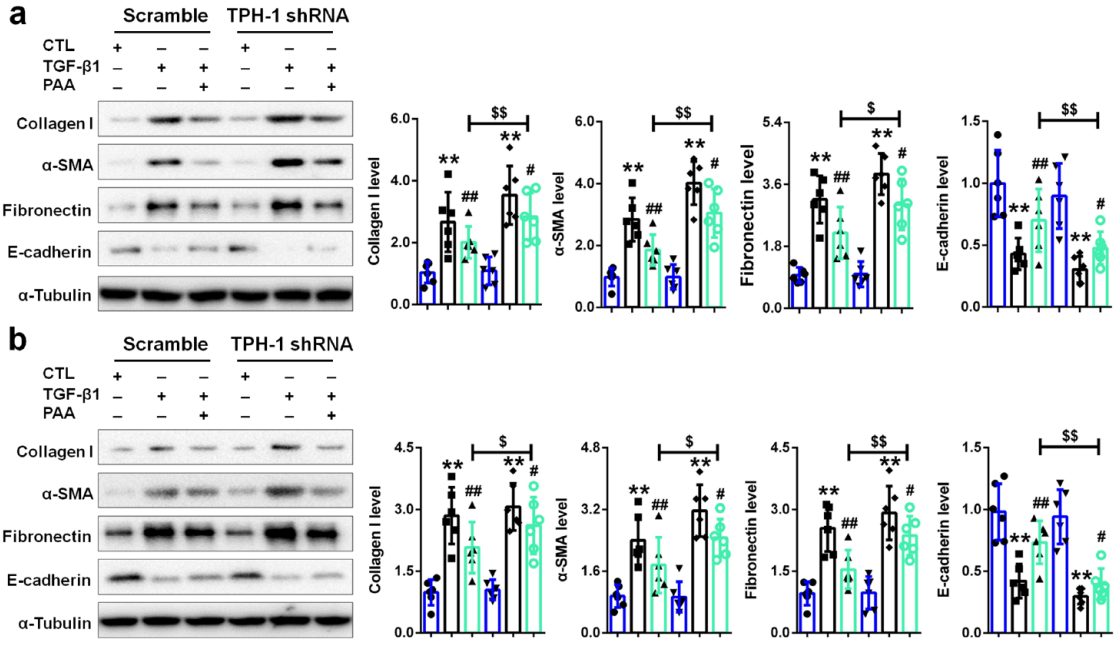

Figure 7. TPH-1 was required for PAA to exert its anti-fibrosis. (a) The protein expression and relative quantitative data of collagen I, α-SMA, fibronectin and E-cadherin in NRK-52E cells. (b) The protein expression and relative quantitative data of collagen I, α-SMA, fibronectin and E-cadherin in NRK-49F cells. Blue, CTL group; black, TGF-β1-treated group; bright green, TGF-β1 + PAA group.
$^{**}p < 0.01$ compared with CTL group ($n = 6$).
$^{\#\#}p < 0.01$ compared with TGF-β1-treated group ($n = 6$).
$^{\$}p < 0.05$.
$^{\$\$}p < 0.01$ compared with TGF-β1 + PAA group after transfected with scramble ($n = 6$).
Dot presented the single data results in the bar graph.
CTL, control; PAA, poricoic acid A; α-SMA, alpha smooth muscle actin; TGF, transforming growth factor; TPH-1, tryptophan hydroxylase-1.

contributed to the anti-fibrotic effects of PAA in NRK-52E and NRK-49F cells indicated by decreased collagen I, fibronectin, α-SMA expression and increased E-cadherin expression. The combined therapy of PAA and TPH-1 overexpression conferred superior renal protection and anti-fibrotic effects than ever when used alone. Accompanied by TPH-1 overexpression, the anti-fibrotic effects of PAA enhanced, indicating that PAA might exert its anti-fibrosis in a TPH-1-dependent manner.

To draw a convincing conclusion that TPH-1 was required for the anti-fibrotic effects of PAA, lentivirus expressing shRNA against rat *Tph1* was further employed. As shown in Figure 7a and b, after knock-down of TPH-1, the anti-fibrotic effects of PAA became weakened indicated by increased collagen I, fibronectin, α-SMA expression and decreased E-cadherin expression in NRK-52E and NRK-49F cells. These results demonstrated that TPH-1 overexpression could enhance anti-fibrotic effects of PAA while TPH-1 deficiency weakened anti-fibrotic effects of PAA, which confirmed that TPH-1 was required for anti-fibrotic effects of PAA. Taken together, PAA as a modulator of TPH-1 expression to inhibit renal fibrosis through regulating the Wnt/β-catenin signaling by acting on the protein stability of β-catenin and β-catenin-mediated transcription (Figure 8). In addition, TPH-1 had the potential to be a therapeutic target against renal fibrosis.

Discussion

Renal fibrosis is a common feature of CKD and results in the loss of kidney function.[31,32] Clinically, angiotensin receptor blocker and angiotensin-converting enzyme inhibitor are the first-line therapy in CKD.[33–36] Even if they could inhibit renal fibrosis, they have some non-negligible side effects and are invalid in certain circumstances.[37] In addition, few drugs target fibrogenesis specifically, which is hindered by the

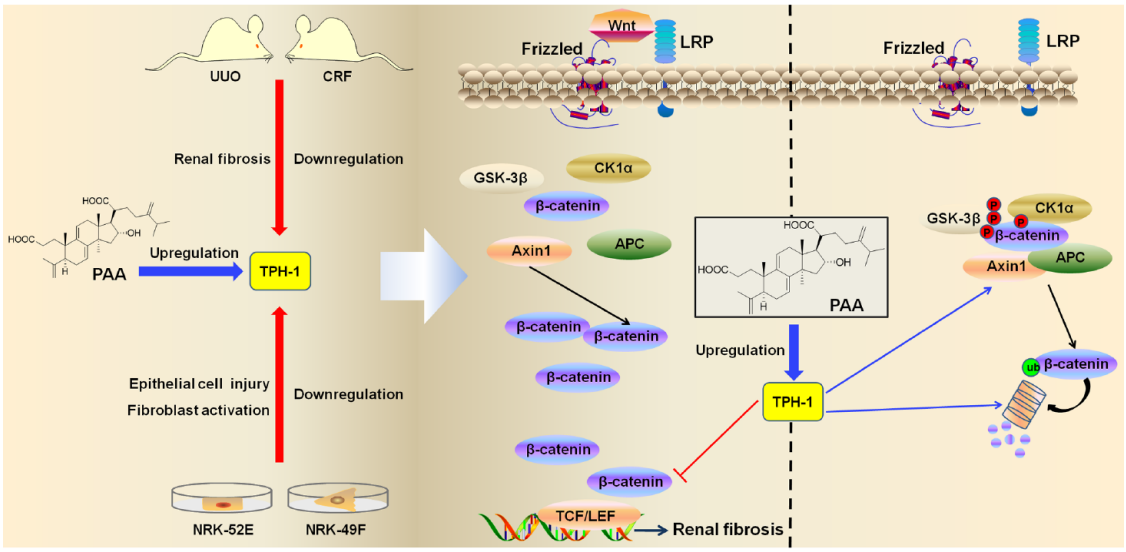

Figure 8. Schematic diagram depicting the effects and mechanisms of TPH-1 against renal fibrosis and the regulation of PAA on TPH-1 expression. TPH-1 was decreased during renal fibrosis, while PAA treatment significantly inhibited renal fibrosis through promoting TPH-1 expression. Pharmacological overexpression of TPH-1 by PAA treatment ameliorated renal fibrosis through modulating the Wnt/β-catenin signaling pathway by acting on the protein stability of β-catenin and β-catenin-mediated transcription. TPH-1 was required for PAA to exert anti-fibrosis.
PAA, poricoic acid A; TPH-1, tryptophan hydroxylase-1.

lack of an effective therapeutic target. Hence, it is urgent to develop the effective therapeutic strategy that directly inhibits fibrosis.

Tryptophan metabolism is closely associated with renal fibrosis.[16,38,39] The dysfunction of tryptophan metabolism was involved in CKD and renal fibrosis.[40–42] Our previous studies have revealed the decreased tryptophan levels and increased levels of tryptophan metabolites including indoxyl sulfate, kynurenine, hippuric acid and 4-aminohippuric acid in plasma, while the increased tryptophan levels and the decreased levels of four metabolites were observed in urine from patients with end-stage renal disease.[43] Tryptophan can be transformed into indoxyl sulfate that further leads to renal fibrosis.[44,45] Tryptophan can also be transformed into indole-3-acetic acid that contributes to kidney dysfunction and increasesd the risk of cardiovascular events in CKD.[46,47] In contrast, a number of metabolites such as tryptanthrin play a renoprotective role.[48] Notably, tryptophan can be transformed into two beneficial metabolites by TPH, and our recent studies indicated the two metabolites, 5-MTP and melatonin, exhibited a renoprotective role in CKD.[10,11,16] Both TPH-1 and TPH-2 convert tryptophan to 5-hydroxytryptophan (5-HTP). Depending on the cell type, 5-HTP is further converted by other enzymes to serotonin or 5-MTP. Serotonin is further converted to melatonin mainly in the pineal gland.[49] Melatonin inhibited inflammation *via* regulating the Gas6/Axl-NF-κB/Nrf2 axis, and suppressed renal fibrosis *via* regulating the interaction of Smad3 and the β-catenin pathway.[10,11] Compared with melatonin, studies about 5-MTP in the kidney are few. Our latest studies identified several metabolites as biomarkers for progressive CKD, including 5-MTP.[16] 5-MTP was decreased in CKD, and supplementation with 5-MTP delayed CKD progression and suppressed renal inflammation,[16] indicating the renoprotective effects of 5-MTP. TPH-1 is an enzyme that initiates tryptophan transformation into 5-HTP, which next is converted to 5-MTP by hydroxyindole O-methyltransferase.[50] TPH-1 is the first enzyme in the 5-MTP biosynthesis pathway.[14,50,51] Knock-in of TPH-1 could increase 5-MTP expression and exert its anti-inflammatory effects *via* regulating the NF-κB/Nrf2 pathway.[16] These results indicated that TPH-1 exerted anti-inflammatory effects and might have the potential to be developed as a therapeutic target in treating renal fibrosis.

In the present study, we found that TPH-1 was gradually impaired during CKD progression,

while PAA treatment significantly promoted TPH-1 expression to inhibit renal fibrosis. PAA is the major component isolated from *P. cocos*, which possesses multiple pharmacological activities including diuretic, renoprotective, lipid-lowering and anti-inflammatory effects.[52–55] Our previous studies have demonstrated the anti-fibrotic effects of PAA,[10–12] and also revealed that PAA could inhibit the Wnt/β-catenin signaling pathway, but the underlying mechanisms remained unclear. The present study demonstrated that PAA treatment could upregulate TPH-1 expression. TPH-1 overexpression by PAA treatment suppressed the Wnt/β-catenin signaling pathway *via* modulating the protein stability of β-catenin and its interaction with TCF4. In addition, TPH-1 was required for PAA to exert its anti-fibrosis. After knock-in of TPH-1, the anti-fibrotic effects of PAA exhibited better than PAA treatment only, while TPH-1 deficiency weakened the anti-fibrotic effects of PAA, indicating that TPH-1 was required for the anti-fibrotic effects of PAA.

To clarify the underlying mechanisms of PAA in modulating TPH-1 expression and Wnt/β-catenin signaling activity, we explored the mechanisms underlying the anti-fibrotic and renoprotective effects of TPH-1. TPH-1 deficiency promoted epithelial cell injury and fibroblast activation, while TPH-1 overexpression inhibited epithelial cell injury and fibroblast activation to attenuate renal fibrosis. Next, we explored the underlying mechanisms. TPH-1 deficiency contributed to renal fibrosis that was associated with the activation of the Wnt/β-catenin signaling pathway. TPH-1 overexpression suppressed Wnt/β-catenin signaling activity, while TPH-1 deficiency promoted Wnt/β-catenin signaling activity. These results pointed to the inhibition of TPH-1 on Wnt/β-catenin signaling activity. Further studies indicated that TPH-1 not only affected the protein stability of β-catenin but also inhibited its interaction with TCF4 and downstream gene expression. These results confirmed that TPH-1 had the potential to be developed as a therapeutic target for renal fibrosis and CKD, and illuminated its underlying mechanisms. Taken together, PAA could promote TPH-1 expression to ameliorate fibrosis through regulating the Wnt/β-catenin signaling pathway. However, our current study has several limitations. Although the present study identified TPH-1 as the therapeutic target of PAA, further studies are still needed to provide direct evidence by using indicated surface plasmon resonance and mutation of the TPH-1-binding site method in the future.

In conclusion, the present study identified PAA as a modulator of TPH-1 expression to suppress renal fibrosis through regulating the Wnt/β-catenin signaling pathway by acting on the protein stability of β-catenin and β-catenin-mediated transcription. TPH-1 was required for anti-fibrotic effects of PAA. In addition, TPH-1 had the potential to be developed as a promising therapeutic target for renal fibrosis and CKD.

Author contributions

DQC and YYZ designed the experiments. DQC, LC, HHH and YNW performed the experiments. DQC analyzed the data. DQC wrote the initial draft of the manuscript. DQC, YYZ and XQW revised the final version.

Conflict of interest statement

The authors declare that there is no conflict of interest.

Funding

The authors disclosed receipt of the following financial support for the research, authorship, and/or publication of this article: This study was supported by the National Natural Science Foundation of China (nos. 81872985 and 81673578), National Key Research and Development Project (no. 2019YFC1709405) and Shaanxi Key Science and Technology Plan Project (no. 2019ZDLSF04-04-02). No funding bodies had any role in the study design, data collection and analysis, decision to publish, or preparation of the manuscript.

ORCID iD

Ying-Yong Zhao https://orcid.org/0000-0002-0239-7342

Supplemental material

Supplemental material for this article is available online.

References

1. Jha V, Garcia-Garcia G, Iseki K, *et al.* Chronic kidney disease: global dimension and perspectives. *Lancet* 2013; 382: 260–272.

2. Levin A, Tonelli M, Bonventre J, *et al.* Global kidney health 2017 and beyond: a roadmap for closing gaps in care, research, and policy. *Lancet* 2017; 390: 1888–1917.
3. Chen DQ, Hu HH, Wang YN, *et al.* Natural products for the prevention and treatment of kidney disease. *Phytomedicine* 2018; 50: 50–60.
4. Nastase MV, Zeng-Brouwers J, Wygrecka M, *et al.* Targeting renal fibrosis: mechanisms and drug delivery systems. *Adv Drug Deliver Rev* 2018; 129: 295–307.
5. Chen DQ, Feng YL, Cao G, *et al.* Natural products as a source for antifibrosis therapy. *Trends Pharmacol Sci* 2018; 39: 937–952.
6. Chen L, Yang T, Lu DW, *et al.* Central role of dysregulation of TGF-β/Smad in CKD progression and potential targets of its treatment. *Biomed Pharmacother* 2018; 101: 670–681.
7. Wang YZ, Zhang J, Zhao YL, *et al.* Mycology, cultivation, traditional uses, phytochemistry and pharmacology of *Wolfiporia cocos* (Schwein). Ryvarden et Gilb: a review. *J Ethnopharmacol* 2013; 147: 265–276.
8. Wang M, Chen DQ, Wang MC, *et al.* Poricoic acid ZA, a novel RAS inhibitor, attenuates tubulo-interstitial fibrosis and podocyte injury by inhibiting TGF-β/Smad signaling pathway. *Phytomedicine* 2017; 36: 243–253.
9. Chen L, Cao G, Wang M, *et al.* The matrix metalloproteinase-13 inhibitor poricoic acid ZI ameliorates renal fibrosis by mitigating epithelial-mesenchymal transition. *Mol Nutr Food Res*. Epub ahead of print 29 March 2019. DOI: 10.1002/mnfr.201900132
10. Chen D, Feng Y, Chen L, *et al.* Poricoic acid A enhances melatonin inhibition of AKI-to-CKD transition by regulating Gas6/Axl-NF-κB/Nrf2 axis. *Free Radical Bio Med* 2019; 134: 484–497.
11. Chen DQ, Cao G, Zhao H, *et al.* Combined melatonin and poricoic acid A inhibits renal fibrosis through modulating the interaction of Smad3 and β-catenin pathway in AKI-to-CKD continuum. *Ther Adv Chronic Dis* 2019; 10: 2040622319869116.
12. Chen DQ, Wang YN, Vaziri ND, *et al.* Poricoic acid A activates AMPK to attenuate fibroblast activation and abnormal extracellular matrix remodelling in renal fibrosis. *Phytomedicine* 2020; 72: 153232.
13. Lovisa S, LeBleu VS, Tampe B, *et al.* Epithelial-to-mesenchymal transition induces cell cycle arrest and parenchymal damage in renal fibrosis. *Nat Med* 2015; 21: 998–1009.
14. Wang YF, Hsu YJ, Wu HF, *et al.* Endothelium-derived 5-methoxytryptophan is a circulating anti-inflammatory molecule that blocks systemic inflammation. *Circ Res* 2016; 119: 222–236.
15. Cheng HH, Kuo CC, Yan JL, *et al.* Control of cyclooxygenase-2 expression and tumorigenesis by endogenous 5-methoxytryptophan. *Proc Natl Acad Sci USA* 2012; 109: 13231.
16. Chen DQ, Cao G, Chen H, *et al.* Identification of serum metabolites associating with chronic kidney disease progression and anti-fibrotic effect of 5-methoxytryptophan. *Nat Commun* 2019; 10: 1476.
17. Edeling M, Ragi G, Huang S, *et al.* Developmental signalling pathways in renal fibrosis: the roles of Notch, Wnt and Hedgehog. *Nat Rev Nephrol* 2016; 12: 426–439.
18. Hurcombe JA, Hartley P, Lay AC, *et al.* Podocyte GSK3 is an evolutionarily conserved critical regulator of kidney function. *Nat Commun* 2019; 10: 403.
19. Feng YL, Chen H, Chen DQ, *et al.* Activated NF-κB/Nrf2 and Wnt/β-catenin pathways are associated with lipid metabolism in CKD patients with microalbuminuria and macroalbuminuria. *BBA Mol Basis Dis* 2019; 1865: 2317–2332.
20. Chen L, Chen DQ, Wang M, *et al.* Role of RAS/Wnt/β-catenin axis activation in the pathogenesis of podocyte injury and tubulo-interstitial nephropathy. *Chem-Biol Interact* 2017; 273: 56–72.
21. Xiang X, Cai HD, Su SL, *et al.* Salvia miltiorrhiza protects against diabetic nephropathy through metabolome regulation and wnt/β-catenin and TGF-β signaling inhibition. *Pharmacol Res* 2019; 139: 26–40.
22. Guo Q, Zhong W, Duan A, *et al.* Protective or deleterious role of Wnt/β-catenin signaling in diabetic nephropathy: an unresolved issue. *Pharmaco Res* 2019; 144: 151–157.
23. MacDonald BT, Tamai K and He X. Wnt/β-catenin signaling: components, mechanisms, and diseases. *Dev Cell* 2009; 17: 9–26.
24. Nusse R and Clevers H. Wnt/β-catenin signaling, disease, and emerging therapeutic modalities. *Cell* 2017; 169: 985–999.
25. Zhang ZH, Vaziri ND, Wei F, *et al.* An integrated lipidomics and metabolomics reveal nephroprotective effect and biochemical mechanism of *Rheum officinale* in chronic renal failure. *Sci Rep* 2016; 6: 22151.
26. Zhang ZH, Wei F, Vaziri ND, *et al.* Metabolomics insights into chronic kidney

disease and modulatory effect of rhubarb against tubulointerstitial fibrosis. *Sci Rep* 2015; 5: 14472.

27. Zhang ZH, Li MH, Liu D, *et al*. Rhubarb protect against tubulointerstitial fibrosis by inhibiting TGF-β/Smad pathway and improving abnormal metabolome in chronic kidney disease. *Front Pharmacol* 2018; 9: 1029.
28. Zhao YY, Feng YL, Bai X, *et al*. Ultra performance liquid chromatography-based metabonomic study of therapeutic effect of the surface layer of *Poria cocos* on adenine-induced chronic kidney disease provides new insight into anti-fibrosis mechanism. *PLoS One* 2013; 8: e59617.
29. Wang M, Chen DQ, Chen L, *et al*. Novel inhibitors of the cellular renin–angiotensin system components, poricoic acids, target Smad3 phosphorylation and Wnt/β-catenin pathway against renal fibrosis. *Br J Pharmacol* 2018; 175: 2689–2708.
30. Chen H, Yang T, Wang MC, *et al*. Novel RAS inhibitor 25-O-methylalisol F attenuates epithelial-to-mesenchymal transition and tubulo-interstitial fibrosis by selectively inhibiting TGF-β-mediated Smad3 phosphorylation. *Phytomedicine* 2018; 42: 207–218.
31. Ma SX, Shang YQ, Zhang HQ, *et al*. Action mechanisms and therapeutic targets of renal fibrosis. *J Nephrol Adv* 2018; 1: 4–14.
32. Xu X, Tan X, Tampe B, *et al*. High-fidelity CRISPR/Cas9-based gene-specific hydroxymethylation rescues gene expression and attenuates renal fibrosis. *Nat Commun* 2018; 9: 3509.
33. Yang T, Chen YY, Liu JR, *et al*. Natural products against renin–angiotensin system for antifibrosis therapy. *Eur J Med Chem* 2019; 179: 623–633.
34. Zuo Y, Li T and Lei Z. Should we add atorvastatin to irbesartan for improving renoprotective effects in early diabetic nephropathy? A meta-analysis of randomized controlled trials. *Pharmacol Res* 2019; 146: 104286.
35. Kumar N and Yin C. The anti-inflammatory peptide Ac-SDKP: synthesis, role in ACE inhibition, and its therapeutic potential in hypertension and cardiovascular diseases. *Pharmacol Res* 2018; 134: 268–279.
36. Takezako T, Unal H, Karnik SS, *et al*. The non-biphenyl-tetrazole angiotensin AT1 receptor antagonist eprosartan is a unique and robust inverse agonist of the active state of the AT1 receptor. *Br J Pharmacol* 2018; 175: 2454–2469.
37. Georgianos PI and Agarwal R. Revisiting RAAS blockade in CKD with newer potassium-binding drugs. *Kidney Int* 2018; 93: 325–334.
38. Chen L, Chen DQ, Liu JR, *et al*. Unilateral ureteral obstruction causes gut microbial dysbiosis and metabolome disorders contributing to tubulointerstitial fibrosis. *Exp Mol Med* 2019; 51: 38.
39. Roager HM and Licht TR. Microbial tryptophan catabolites in health and disease. *Nat Commun* 2018; 9: 3294.
40. Zhao YY, Cheng XL, Wei F, *et al*. Serum metabonomics study of adenine-induced chronic renal failure in rats by ultra performance liquid chromatography coupled with quadrupole time-of-flight mass spectrometry. *Biomarkers* 2012; 17: 48–55.
41. Wang YN, Ma SX, Chen YY, *et al*. Chronic kidney disease: biomarker diagnosis to therapeutic targets. *Clinica Chim Acta* 2019; 499: 54–63.
42. Zhao YY. Metabolomics in chronic kidney disease. *Clinica Chim Acta* 2013; 422: 59–69.
43. Chen DQ, Cao G, Chen H, *et al*. Gene and protein expressions and metabolomics exhibit activated redox signaling and Wnt/β-catenin pathway are associated with metabolite dysfunction in patients with chronic kidney disease. *Redox Biol* 2017; 12: 505–521.
44. Agus A, Planchais J and Sokol H. Gut microbiota regulation of tryptophan metabolism in health and disease. *Cell Host Microbe* 2018; 23: 716–724.
45. Chen YY, Chen DQ, Chen L, *et al*. Microbiome-metabolome reveals the contribution of gut–kidney axis on kidney disease. *J Transl Med* 2019; 17: 5.
46. Dou L, Sallée M, Cerini C, *et al*. The cardiovascular effect of the uremic solute indole-3 acetic acid. *J Am Soc Nephrol* 2015; 26: 876.
47. Song P, Ramprasath T, Wang H, *et al*. Abnormal kynurenine pathway of tryptophan catabolism in cardiovascular diseases. *Cell Mol Life Sci* 2017; 74: 2899–2916.
48. Zhang X, Xia J, Zhang W, *et al*. Study on pharmacokinetics and tissue distribution of single dose oral tryptanthrin in Kunming mice by validated reversed-phase high-performance liquid chromatography with ultraviolet detection. *Integr Med Res* 2017; 6: 269–279.
49. Wu KK, Cheng HH and Chang TC. 5-Methoxyindole metabolites of L-tryptophan:

control of COX-2 expression, inflammation and tumorigenesis. *J Biomed Sci* 2014; 21: 17.

50. Chu LY, Wang YF, Cheng HH, *et al*. Endothelium-derived 5-methoxytryptophan protects endothelial barrier function by blocking p38 MAPK activation. *PLoS One* 2016; 11: e0152166.
51. Cheng HH, Chu LY, Chiang LY, *et al*. Inhibition of cancer cell epithelial mesenchymal transition by normal fibroblasts via production of 5-methoxytryptophan. *Oncotarget* 2016; 7: 31243–31256.
52. Zhao YY, Feng YL, Du X, *et al*. Diuretic activity of the ethanol and aqueous extracts of the surface layer of *Poria cocos* in rat. *J Ethnopharmacol* 2012; 144: 775–778.
53. Feng YL, Lei P, Tian T, *et al*. Diuretic activity of some fractions of the epidermis of *Poria cocos*. *J Ethnopharmacol* 2013; 150: 1114–1118.
54. Zhao YY, Lei P, Chen DQ, *et al*. Renal metabolic profiling of early renal injury and renoprotective effects of *Poria cocos* epidermis using UPLC Q-TOF/HSMS/MSE. *J Pharm Biomed Anal* 2013; 81–82: 202–209.
55. Miao H, Zhao YH, Vaziri ND, *et al*. Lipidomics biomarkers of diet-induced hyperlipidemia and its treatment with *Poria cocos*. *J Agr Food Chem* 2016; 64: 969–979.